In vitro and In vivo Degradation Evaluation of Mg-Based Alloys for Biomedical Applications

Sau Shun Wong[1,*], Luen Chow Chan[2], Chi Ping Lai[2], Wing Yuk Ip[1] and Lok Hang Chau[2]

[1]*Department of Orthopaedics and Traumatology, 5/F Professional Block, The University of Hong Kong, Queen Mary Hospital, Hong Kong, China*

[2]*Department of Industrial and Systems Engineering, The Hong Kong Polytechnic University, Hung Hom, Kowloon, Hong Kong, China*

Abstract: Biodegradable metals have attracted interest for implant applications because of the potential to eliminate secondary surgeries. Magnesium-based (Mg-based) alloys are potential candidates. The purpose of this study was to evaluate the *in vitro* and *in vivo* degradation performances of two custom-made magnesium-based alloys and to determine whether they are sustainable for further investigation. The performances of Magnesium-Zinc-Manganese (Mg-Zn-Mn) alloys at 5% and 1% zinc levels were compared using a mechanical test, hydrogen evolution test, cell viability (MTT) test, and a short term mice subcutaneous implantation. The results showed that the corrosion resistance of the Mg was improved by alloying. While Mg-5Zn-1Mn was more corrodible compared with Mg-1Zn-1Mn, neither of the alloys presented any adverse effects preliminarily and both were suitable for long-term testing for biomedical applications.

Keywords: Biodegradable, magnesium, *in vivo,* hydrogen gas, zinc.

1. INTRODUCTION

Current metallic implants for bone fixation present problems as they require secondary surgery for removal. A large portion of elective orthopaedic operations involves the removal of fixation devices [1,2]. Revision surgery hence increases the medical costs as well as the health risks for patients. The development of absorbable orthopaedic devices aims to lower these medical expenses, and evidence has shown that total medical expenses were lower when using absorbable (polymer) orthopaedic devices compared with traditional non-absorbable metallic devices [3-7].

An ideal bioresorbable orthopaedic implant should provide adequate mechanical support that matches the bone healing process and resorbs progressively [8]. Magnesium has an elastic modulus (41-45GPa) and density (1.74-2.0g cm^{-3}) that are similar to bones (3-20GPa, 1.8-2.1g cm^{-3}), which are quite biomechanically compatible [9]. The potential of Mg implants has been acknowledged in the past decades because of its high weight-strength ratio and low toxicity [10,11].

The biodegradation of magnesium means its *in vivo* corrosion. Under atmospheric conditions, an oxide film of magnesium hydroxide is formed spontaneously on the unprotected magnesium. The oxide layer protects the magnesium from further corrosion and is slightly soluble in water. Hydrogen gas is evolved as a by-product. The hydrogen gas is suspected to be the cause of the formation of *in vivo* gas cavities, which were reported in literature [12]. When the magnesium is immersed in an aqueous environment with a high level of chloride ions (e.g. physiological environment), the magnesium hydroxide reacts with the chloride ions and forms the highly soluble magnesium chloride [13].

The reaction of magnesium in an aqueous environment:

$$Mg(s) + 2H_2O(l) \rightarrow Mg(OH)_2(s) + H_2(g)$$

The reactions of magnesium in an environment with a high chloride level:

$$Mg(s) + 2Cl^-(aq) \rightarrow MgCl_2(s)$$

$$Mg(OH)_2(s) + 2Cl^-(aq) \rightarrow MgCl_2(s)$$

In order to adjust the corrosion rate of magnesium, modifications such as metal working, alloying, and coating are commonly performed to improve magnesium's corrosion resistance [14-16]. It is known that the addition of zinc (Zn) and manganese (Mn) can increase the mechanical strength and corrosion resistance for the conventional metal alloys. Through the solution hardening mechanism, the grain size of the Mg alloys is refined by the addition of the Zn element. The mechanical properties, such as tensile strength and yield strength, can be improved effectively [17-19]. On the other hand, Mn is used commonly as an alloying element to remove impurities in alloys [20].

*Address correspondence to this author at the Department of Orthopaedics and Traumatology, 5/F Professional Block, The University of Hong Kong, Queen Mary Hospital, Hong Kong, China; Tel: +852 39179594;
Fax: +852 28185210; E-mail: wss.alicia@gmail.com

E-ISSN: 2410-4701/15

Biodegradation studies using Mg alloys with different amounts of Zn and Mn additions have demonstrated promising results. The typical range of zinc addition to magnesium alloy is from 1% to 5% for mechanical enhancement. [2,15-19] The best corrosion resistance has been found at 1% zinc addition, but the corrosion property decreased when the zinc content was beyond 3% [19]. Therefore, Mg alloys with 1% and 5% Zn (and fixed amount of 1% Mn) were the focus of the current study. A difference in corrosion resistances was expected. Meanwhile, the content of manganese was kept constant at 1% to limit the number of experimental variables. The performances of magnesium-zinc-manganese (Mg-Zn-Mn) alloys at 5% and 1% zinc levels were compared by *in vitro* and *in vivo* methods.

2. MATERIALS AND METHODS

2.1. Materials Production

Ti-6Al-4V, 99.999% Pure Mg, Mg-5Zn-1Mn, and Mg-1Zn-1Mn alloys were produced in forms of rods of 10mm diameter by hot extrusion. The samples were then prepared into different sizes and shapes for different tests as listed in Table **1**. Before the experiments, all the samples were immersed in 35% chromic acid (H_2CrO_4) to remove the oxide formed on their surfaces. They were cleaned in acetone and ethanol sonication before use. The compositions of the samples were verified by energy-dispersive X-ray spectroscopy (EDX) using the Hitachi S-3400N Variable Pressure Scanning Electron Microscope as shown in Table **2**.

2.2. Mechanical Test

The tensile test was set up according to ASTM E8 [21]. Specimens of 6 mm gauge width and 38 mm gauge length were used. The test was conducted under a speed of 1mm/min at room temperature using the 810 Material Test System (MTS).

2.3. Hydrogen Evolution Test

The sample discs were mounted in epoxy, as shown in Figure **1**. Then the samples were immersed individually in Ringer's solution for~350 hours (>14

Table 1: Specifications and Diagrams of the Test Samples

Test	Shape	Specifications	Schematic*
Tensile test	"dumbbell"	6mm gauge width, 38mm gauge length	
Hydrogen evolution test	disc	10mm diameter, 3 mm thickness	
Cell viability test (MTT)	disc	10mm diameter, 3 mm thickness	
Animal test	rod	1.6mm diameter, 3 to 4mm length	

*Schematics not drawn to scale.

Table 2: EDX Results for the Cleaned Discs. The Weight Percent (wt%) of each element in the discs are shown

	Mg	Zn	Mn	C	O
Mg-1Zn-1Mn	96.56	0.89	1.03	<0.8	0
Mg-5Zn-1Mn	91.03	4.98	1.13	< 1	<0.5

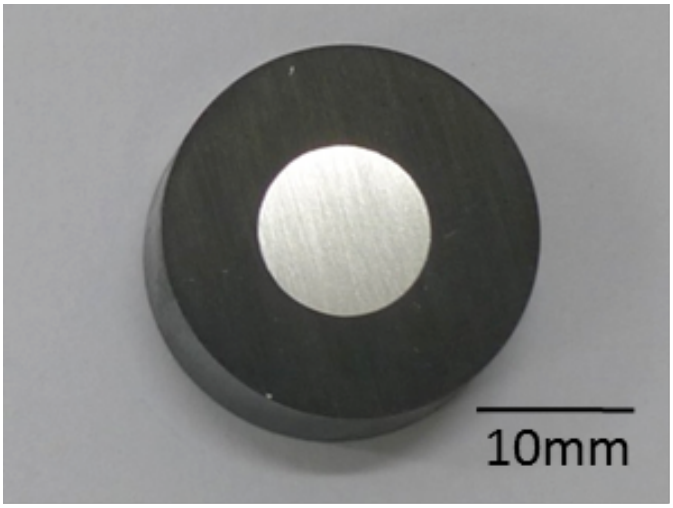

Figure 1: Disc sample mounted in epoxy.

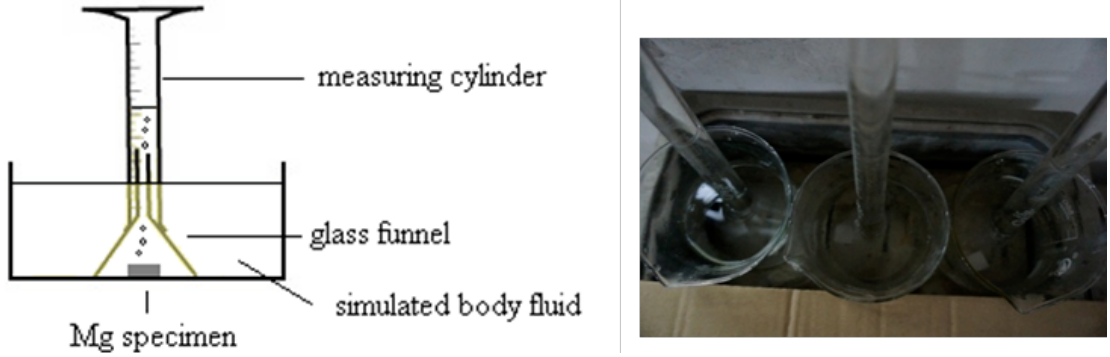

Figure 2: Schematic (left) and photo (right) of the hydrogen evolution test set-up.

days) at 37 degrees Celsius at the set-up shown in Figure **2**. The hydrogen gas was collected by the displacement of the solution and was recorded at multiple time points over the immersion period.

2.4. Cell Viability Test by MTT Assay

Three samples of each alloy (Mg-1Zn-1Mn, Mg-5Zn-1Mn, and Ti-6Al-4V) were used in the test. Titanium alloy was used as the positive control representing a foreign non-cytotoxic alloy.

The samples were divided into three groups representing three time-points (t=8, 24, 48hr). The extracts were prepared by immersing the samples individually in (Dulbecco's Modified Eagle's medium) DMEM with 10% FBS (1 mL per 0.2g sample) in a 12-well cell culture plate. The immersion took place at 37 degrees Celsius in 5% CO_2 incubator. The extracts were then collected and frozen at 4 degrees Celsius until use.

Human osteosarcoma cells (MG-63) (over 5 passages), at the concentration of 10,000 cells per well, were pre-cultivated in a 96-well cell culture plate until the cell density reached 60% confluency. The medium in the cell culture was replaced by the extracts at 0X, 1X, 2X and 5X dilutions. The cell culture was incubated at 37 degrees Celsius in the 5% CO_2 incubator for another 72 hours before the cell viability test. Thiazoylblyetetrazolium bromide (98%) and sodium dodecyl sulphate BioXtra (>99.0%) were purchased from Sigma-Aldrich. The test was performed following the protocol published by Sigma Aldrich for the *In vitro* Toxicology Assay Kit, MTT based. The Multiskan GO Microplate Spectrophotometer (Thermo Scientific) and the SkanIt Software (Thermo Scientific) were used for the measurement and calculation of the data. The colour changes (phenol red as pH indicator) and the gas formation of the medium were also observed. Viability less than 75% indicates potential cytotoxicity [22, 23].

2.5. Short Term Mice Subcutaneous Implantation

The test was modified based on the international standard ASTM F1408. Nine 9-weeks old BALB/C mice

were divided into three groups and each group received one type of implant (99.999% Pure Mg, Mg-1Zn-1Mn, Mg-5Zn-1Mn). The Pure Mg group served as the unalloyed control. Each mouse received one implant subcutaneously at the back. The mice were examined by X-ray imaging at the designated time-points over 15 days. The animal experimental protocol had been approved by the Committee on the Use of Live Animals in Teaching and Research of the University of Hong Kong and local animal research authorities.

The mouse was anesthetized by intraperitoneal injection of a mixture of Katamine (90mg kg^{-1}) and Xylazine (10mg kg^{-1}). After the skin preparation and sterilization procedure, a 1cm long subcutaneous incision was made away from the implantation site (middle of the back) on the midline. A tunnel was made along the midline towards the implantation site. The implant was pushed longitudinally through the tunnel to the designated implantation site. The wound was then sutured. After the surgery, all the mice were allowed to move without external support.

The cross-section of the gas cavity of each mouse was examined by the X-ray imaging on days 0, 1, 4, 7, 11, 13, and 15. The cross-sectional area of the gas pocket was measured by the image processing program Image J.

At the end-point of the experiment, the mice were euthanized by penobarbitol (Dorminal) through intraperitoneal injection. Pictures of the implantation locations were taken.

3. RESULTS

3.1. Mechanical Properties of Mg-Zn-Mn Alloys

Table **3** shows a comparison of the tensile strengths of the Mg alloys, commercial Ti alloys, stainless steel and animal bones. The difference between the Mg-5Zn-1Mn and the Mg-1Zn-1Mn alloys was small, which was only 8MPa. Compared with the Ti alloys and stainless steel, the Mg alloys demonstrated the tensile strengths that were more similar to those of the bones.

3.2. Hydrogen Evolution Test

As illustrated in Figure **3**, both alloys released hydrogen gas steadily over the immersion period. No abrupt change in gas release was recorded. The corrosion rate of Mg-5Zn-1Mn was higher, indicated by the steeper slope in the Figure. The appearance of the samples also changed along the immersion period as

Table 3: Tensile Strengths of the Mg-1Zn-1Mn and Mg-5Zn-1Mn Alloys, Compared with Available Data for Ti Alloys, Stainless Steel and Cortical Bone Obtained from [13].

Tissue/alloy	Tensile strength (MPa)
Cortical bone	35-283
Titanium (TiAl6V4)	830-1172
Stainless steel 316L	480-620
Mg-1Zn-1Mn	178.78
Mg-5Zn-1Mn	170.14

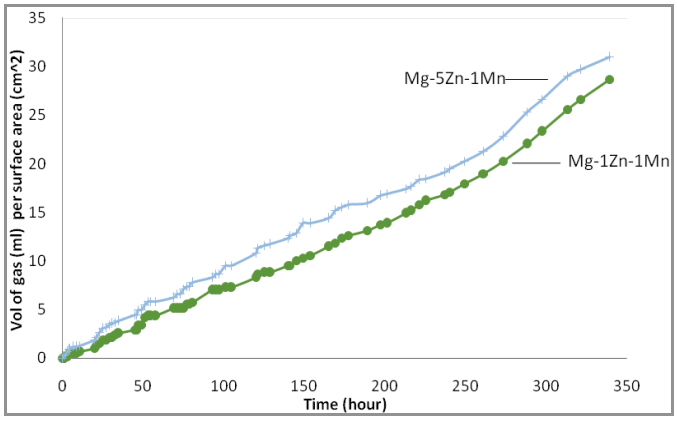

Figure 3: The amount of hydrogen gas evolved from Mg-1Zn-1Mn, Mg-5Zn-1Mn, and Pure Mg samples over 350 hours of immersion in Ringer's solution at 37°C.

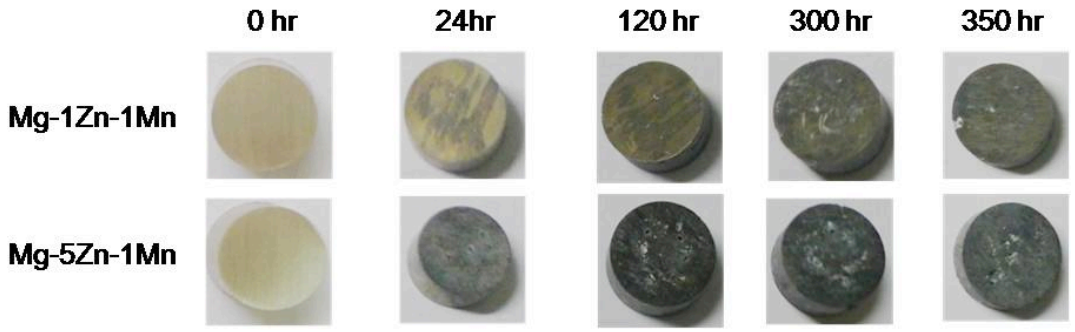

Figure 4: The appearances of the samples at 0hr, 24hr, and 350hr of the immersion test. (All the samples were 10 mm in diameter, and 3 mm in thickness).

illustrated in Figure **4**. For Mg-1Zn-1Mn, the corrosion proceeded slowly and the surface did not turn dark until t=120h. At the end of immersion, the sample was covered by a layer of dark corrosion products and a few white particles were found attaching on the bulk sample. For Mg-5Zn-1Mn, the sample surface was already covered by the corrosion products after 24 hours of immersion. Several shallow pits also appeared. As the immersion time increased, the sample turned darker and some white particles were observed on the surface. Both alloys maintained their structural integrity throughout the immersion period. At the end of the immersion period, a reduction of 0.70% and 0.98% in mass were recorded for Mg-1Zn-1Mn and Mg-5Zn-1Mn respectively.

3.3. Cell Viability Test by MTT Assay

From Figure **5**, it can be seen that the Ti alloy extract was not cytotoxic at all the time-points and dilutions. It served as a control indicating that the cytotoxicity of an inert material would not be affected by

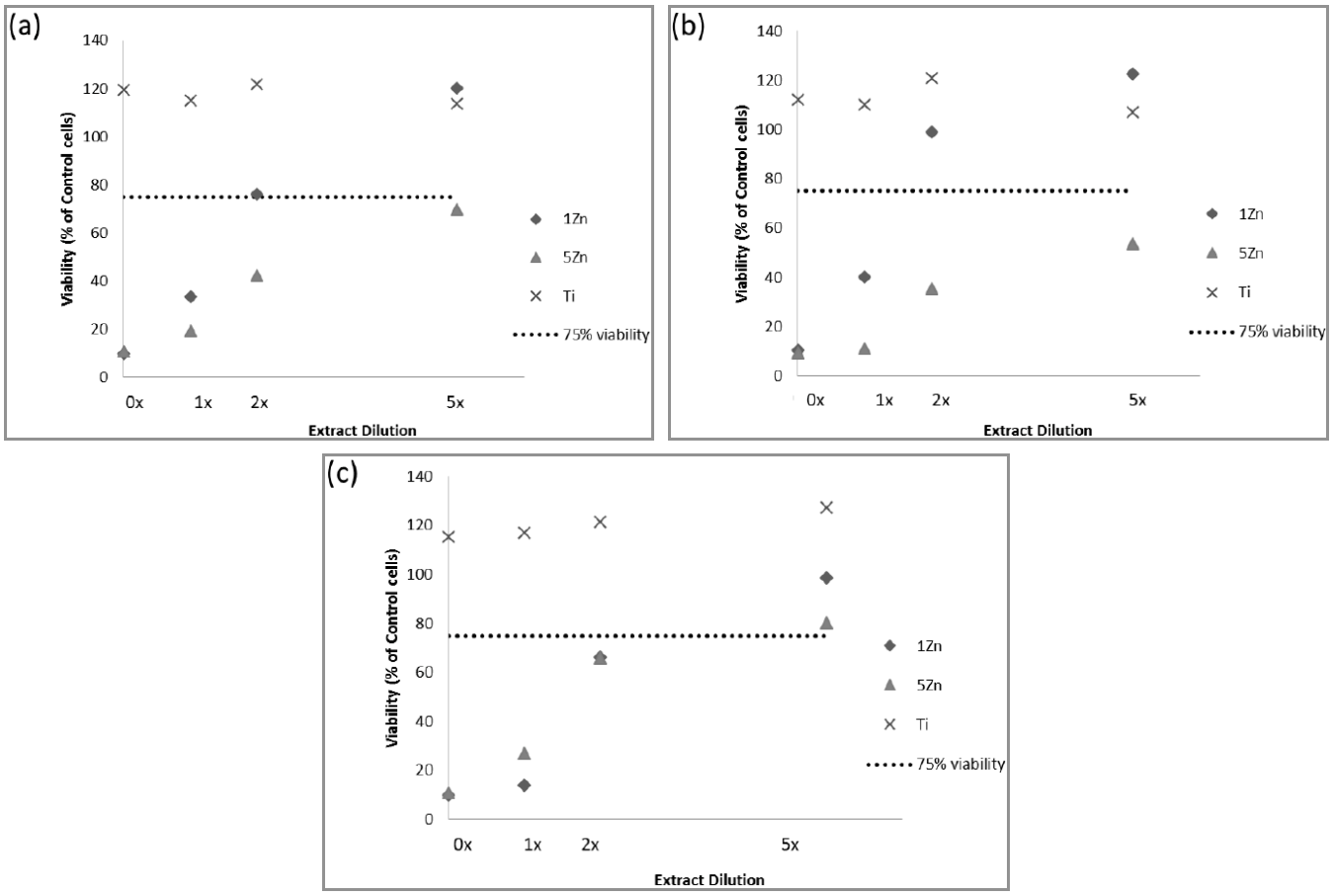

Figure 5(a-c): Viability of the MG-63 cells in 8hrs(**a**), 24hrs(**b**), and 48hrs(**c**) immersion extracts. The data is normalized to the regular DMEM.

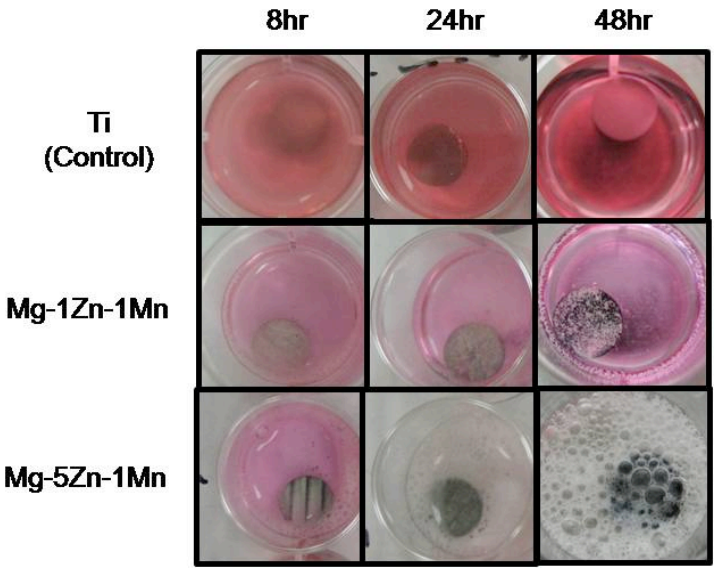

Figure 6: Images of the non-diluted extracts (0X) after 8hr, 24hr and 48hr immersion. All the extracts showed changes in colour except the control (Ti64)'s extract.

the presence, the immersion time, or the extract dilution factor. For the Mg alloys, both the extract dilution and the immersion time posed effects on the cell viability. All the undiluted Mg alloy extracts were cytotoxic with low cell viability varying from 10% to 40%. At 0x dilution, the cell viabilities of both alloys' extracts were too low for comparison. When the extracts became more diluted, an increase in the cell viability was observed and the differences in the cell viabilities became more distinguishable. At 2x and 5x dilutions for all time-points, the cell viability of the Mg-1Zn-1Mn extracts was higher than Mg-5Zn-1Mn extracts. Also, the Mg-5Zn-1Mn extracts were cytotoxic at almost all the time-points and dilutions.

The colour change and the formation of gas bubbles in the medium are shown in Figure **6**. While the Ti64's extract remained the original DMEM's phenol red in colour, the Mg-1Zn-1Mn and Mg-5Zn-1Mn extracts turned pale (alkaline) gradually. An alkaline environment is not desirable for cell survival, which is reflected clearly by the low cell viability results shown in Figure **5**. Gas bubble formation was observed in the Mg-5Zn-1Mn extracts and more gas bubbles were formed as the immersion time increased. The formation of gas bubbles indicated the quick release of gas products, thus a rapid corrosion process. Only a small amount of gas bubbles was found in the Mg-1Zn-1Mn extracts at t=48h, indicating that the corrosion was relatively slow.

3.4. Subcutaneous Implantation

The mice appeared normal and their movements were unaffected by the presence of the gas cavities throughout the experiment. The change in the size of the subcutaneous gas pocket was captured in the X-ray film, as shown in Figure **7**. Figure **8** shows that the

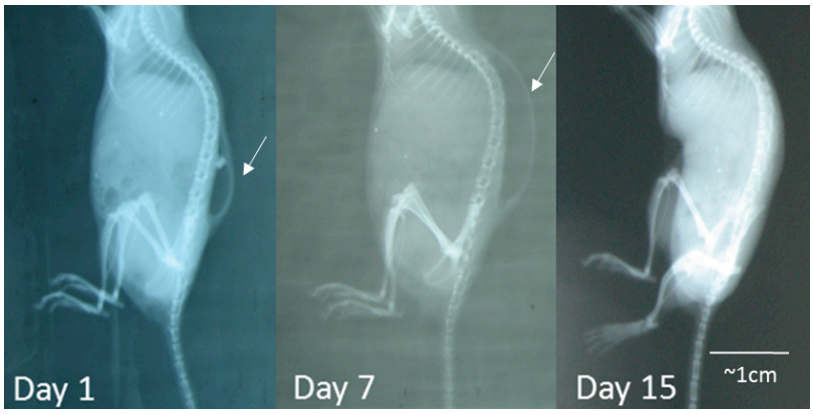

Figure 7: Examples of the X-ray films (day 1, day 7, day 15) of a mouse implanted with Pure Mg. The locations of the gas cavities are indicated by the white arrows.

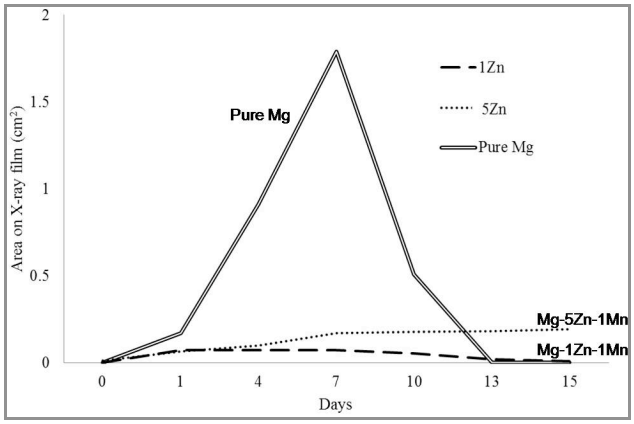

Figure 8: Cross-section areas of the gas cavities shown on the X-ray film over 15 days of subcutaneous implantation.

size of the gas cavity in the mice with the Pure Mg implants (Pure Mg mice) increased rapidly after the implantation. After day 7, the cavities started shrinking rapidly until the total disappearance in day 13. Such rapid gas cavity appearance and disappearance was not observed in the mice with the Mg alloys. As shown in Figure **8**, in the mice with the Mg-5Zn-1Mn implants (5Zn mice), the sizes of the gas cavities increased relatively fast until day 7. After day 7, the increase slowed down but the gas cavities remained. For the mice with the Mg-1Zn-1Mn implants (1Zn mice), the biggest gas cavities were observed on day 1 and the cavities shrank to almost undetectable at the end.

The implantation sites were shaved and the gas cavity locations were exposed as shown in Figure **9**. The skin surfaces were not reddened or ulcerated. For the Pure Mg mice, the gas cavities were not visible on the skin surfaces. For the mice with the Mg alloy implants, their gas cavities were visible and irregularly shaped.

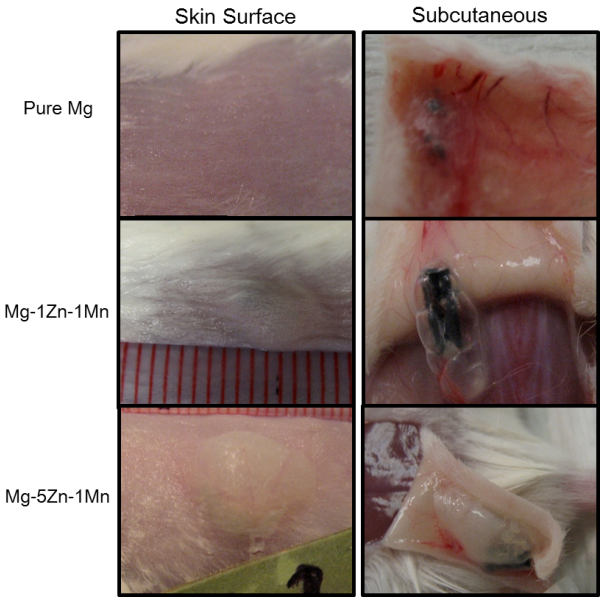

Figure 9: Images of the gas cavities on the surface of the skin (left); implants and gas pocket in subcutaneous layer (right).

The gas cavity at the subcutaneous level can be seen more clearly in the right-hand column of Figure **9**. Instead of a single gas cavity filled with hydrogen gas, it consisted of a combination of several smaller translucent tissue membrane-like gas pockets encapsulating some dark colour debris and/or remaining implants. The implants turned dark because of the oxide layer formation. While the Pure Mg implant had been broken down into pieces, all the other implants maintained their structures. The muscles also appeared to be normal.

4. DISCUSSION

The following discussion will evaluate the potential of Mg-Zn-Mn alloys' for biodegradable implants in terms of their mechanical strength, cytotoxicity, *in vitro* and *in vivo* corrosion properties.

4.1. Enhanced Mechanical Strength

The current study has shown that the Mg-Zn-Mn alloys have mechanical properties that better match with natural bones than traditional orthopaedic titanium alloys. Hence the use of the Mg-Zn-Mn alloys is mechanically more compatible for orthopaedic applications.

4.2. The Addition of Zinc and Corrosion Resistance

In a corrosion-susceptible environment, magnesium suffers from various uniform and localized corrosion attacks. The addition of zinc will improve its corrosion resistance. Nevertheless, the current study has shown that the corrosion resistance will not increase with the zinc composition. The Mg-5Zn-1Mn was more corrodible than the Mg-1Zn-1Mn. This result agrees with that of the previous study, in which the corrosion resistance decreases when the Zn content exceeds 3% in Mg-Zn-Mn alloys [19]. Pits were observed on the alloys' surfaces. Even though the pits were small and shallow, such corrosion pits might penetrate and damage the structural integrity eventually [24].

An ideal degradable implant should be structurally stable at the early stage of fracture because the stability at the wound will determine the bone healing quality [25]. From the *in vitro* immersion test, only less than 1% of mass losses were recorded in the Mg

alloys. In addition, the *in vivo* test observation demonstrated that the structures of the Mg alloy implants were well maintained, while the pure Mg implant was broken down into pieces within two weeks of implantation. The Mg-Zn-Mn alloys were found to be more bio-corrosion resistant.

4.3. Cytotoxicity and Biocompatibility of the Alloys

The major corrosion product of magnesium is magnesium hydroxide, which is not harmful to the human body. It might enhance bone growth temporarily [25,26]. However, the hydrogen gas product from the corrosion process turns the surrounding alkaline gradually and lowers the biocompatibility [12]. The current study showed that the cell viability was affected adversely when the immersion medium became increasingly alkaline. The Mg-5Zn-1Mn was more corrodible, hence more cytotoxic in the current setting. This finding will serve the purpose of comparison but cannot predict the alloy's actual biocompatibility. This is because the *in vivo* corrosion can be about two to three times slower than the *in vitro* corrosion [27].

When the alloys were placed inside the mice, the well-being and the tissues of the hosts did not seem to be affected (by observation). This primary observation indicated that there was no acute or severe host reaction. Hence, it is acceptable for the alloys in the current test to proceed to a more invasive animal test procedure such as bone implantation.

4.4. The Relationship Between Hydrogen Gas Evolution Test and Subcutaneous Implantation

The gap between the steady corrosion behaviour from the hydrogen evolution test and the changing gas cavity size in the *in vivo* study can be bridged by the following assumption.

The difference between the *in vitro* and the *in vivo* corrosion process is that the gas product constantly exchanges with the surrounding tissues *in vivo* whereas such an exchange was not simulated in the *in vitro* set-ups [29]. Therefore, if the gas production rate is slow (e.g. high corrosion resistance, formation of oxide layer, complete degradation, etc.), the gas product will be exchanged instead of accumulating to form a gas pocket.

For the least corrosion resistant pure Mg implant, the rapid corrosion process led to the formation of a gas pocket at the beginning. When the degradation slowed down, the gas exchange became faster than the gas production, hence the gas cavity shrank. For the more corrosion-resistant implant, Mg-1Zn-1Mn, the bio-corrosion was slow and became even slower after the formation of the oxide layer (which protected the Mg from further corrosion attack); therefore the gas cavity remained very small in size at all times. The Mg-5Zn-1Mn was shown to be less corrosion resistant than the Mg-1Zn-1Mn in the hydrogen evolution test, therefore it was within expectations to observe the formation of the larger gas pocket in the implantation site.

4.5. The Meaning of the Short Term Subcutaneous Implantation Test's Finding

The dissection pictures of the subcutaneous layer also revealed the limitation of using the cross-section area measurement. The sizes and the shapes of the gas cavities could be changed easily under mechanical stresses, e.g. tight skin and movements. Therefore, the area of the gas cavities on the X-ray images can only represent an estimation of the gas formation. The trend of the data is more meaningful than the actual value.

5. CONCLUSION

In this study, two magnesium based alloys Mg-1Zn-1Mn and Mg-5Zn-1Mn were custom-made and studied in the mechanical test, the *in vitro* tests, and the *in vivo* tests. The following insights can be concluded from the study based on the results and the observations.

1. The test alloys were mechanically suitable for implantation: The yield strengths of the Mg alloys matched well with the natural bones, therefore the use of the Mg alloys should be able to avoid the stress shielding problem.

2. Mg-1Zn-1Mn showed less hydrogen gas formation in the hydrogen evolution test: Steady increasing gas release behaviours were recorded in the test metals.

3. Cytotoxicity was affected by the alkalinity from the corrosion: The Mg-5Zn-1Mn alloy was more cytotoxic compared with the Mg-1Zn-1Mn as it turned the medium alkaline quickly, which lowers the medium's cell viability.

4. Potential gas exchange *in vivo*: The subcutaneous gas cavities were larger in the Pure Mg than those in the Mg alloys. Since external means were not used to remove the gas, the gas was likely exchanged by diffusion. Gas exchange might occur and reduce the gas cavity size gradually.

From the various tests in this preliminary study, the Mg-5Zn-1Mn and Mg-1Zn-1Mn alloys demonstrated certain improved corrosion resistances and basic biocompatibility for implantation. The Mg-Zn-Mn alloys of different wt % of Zn can be evaluated to determine the effect of Zn on the alloy's biocorrosion performance. Depending on the applications, more simulation tests should be performed to further investigate the mechanical properties of the Mg alloys. Long term animal tests should also be carried out to further investigate the feasibility of using these custom alloys for biomedical applications.

ACKNOWLEGMENTS

The work described in this paper was partially supported by grants from the Innovation and Technology Fund of the Hong Kong Special Administrative Region, China (Project No. ITP/041/12NI), the Research Committee of the Hong Kong Polytechnic University (Project No. G-YL64), and the Small Project Funding of the University of Hong Kong (Project No. 201309176011).

REFERENCES

[1] Bostman O, H Pihlajamaki. Routine implant removal after fracture surgery: a potentially reducible consumer of hospital resources in trauma units. J Trauma 1996; 41 (5): 846-849. PMID: 8913214. http://dx.doi.org/10.1097/00005373-199611000-00013

[2] Kubásek J, Vojtech D. Structural characteristics and corrosion behaviour of biodegradable Mg-Zn, Mg-Zn-Gd alloys. J Mater Sci Mater Med 2013; 24 (7): 1615-1626. http://dx.doi.org/10.1007/s10856-013-4916-3

[3] Bostman O, Hirvensalo E, Partio E, Törmälä P, Rokkanen P. Impact of the use of absorbable fracture fixation implants on consumption of hospital resources and economic costs. J Trauma 1991; 31 (10): 400-1403. PMID: 1942152

[4] Juutilainen T, Pätiälä H, Ruuskanen M, Rokkanen P. Comparison of costs in ankle fractures treated with absorbable or metallic fixation devices. Arch Orthop Trauma Surg 1997; 116(4): 204-208. PMID: 9128772. http://dx.doi.org/10.1007/BF00393710

[5] Bostman OM. Metallic or absorbable fracture fixation devices. A cost minimization analysis. Clin Orthop Relat Res 1996; (329): 233-239. PMID: 8769457. http://dx.doi.org/10.1097/00003086-199608000-00029

[6] Rokkanen PU, Bostman O, Hirvensalo E, Mäkelä EA, Partio EK, Pätiälä H, *et al*. Bioabsorbable fixation in orthopaedic surgery and traumatology. Biomaterials 2000; 21(24): 2607-2613. PMID: 11071610. http://dx.doi.org/10.1016/S0142-9612(00)00128-9

[7] Böstman O, Hirvensalo E, Partio E, Törmälä P, Rokkanen P. Resorbable rods and screws of polyglycolide in stabilizing malleolar fractures. A clinical study of 600 patients. Unfallchirurg 1992; 95(2): 109-112. PMID: 1315079

[8] Witte F. In-Vivo Korrosion von Magnesium legierungen und ihrebiolokishen Effekte: Analysen von Tiermodellen. GKSS, Workshop Magnesium in der Medizin 2005.

[9] Choudhary L, Raman RK. Magnesium alloys as body implants: Fracture mechanism under dynamic and static loadings in a physiological environment. Acta Biomater 2012; 8(2): 916-923. PMID: 22075121. http://dx.doi.org/10.1016/j.actbio.2011.10.031

[10] Song GL, Atrens A. Corrosion Mechanisms of Magnesium Alloys. Adv Eng mater 1999; 1(1): 23. http://dx.doi.org/10.1002/(SICI)1527-2648(199909)1:1<11::AID-ADEM11>3.0.CO;2-N

[11] Yuen CK, Ip WY. Theoretical risk assessment of magnesium alloys as degradable biomedical implants. Acta Biomater 2010; 6(5): 1808-1812. http://dx.doi.org/10.1016/j.actbio.2009.11.036

[12] Kuhlmann J, Bartsch I, Willbold E, Schuchardt S, Holz O, Hort N, *et al*. Fast escape of hydrogen from gas cavities around corroding magnesium implants. Acta Biomater 2013; 9(10): 8714-8721. http://dx.doi.org/10.1016/j.actbio.2012.10.008

[13] Witte F, Hort N, Vogt C, Cohen S, Kainer KU, Willumeit R. Degradable biomaterials based on magnesium corrosion. Curr Opin Solid State Mater Sci 2008; 12(5-6): 10. http://dx.doi.org/10.1016/j.cossms.2009.04.001

[14] Li Z, Gu X, Lou S, Zheng, Y. The development of binary Mg-Ca alloys for use as biodegradable materials within bone. Biomaterials 2008; 29(10): 1329-1344. http://dx.doi.org/10.1016/j.biomaterials.2007.12.021

[15] Rosalbino F, De Negri S, Saccone A, Angelini E, Delfino S. Bio-corrosion characterization of Mg-Zn-X (X = Ca, Mn, Si) alloys for biomedical applications. J Mater Sci Mater Med 2010; 21(4): 1091-1098. http://dx.doi.org/10.1016/j.biomaterials.2007.12.021

[16] Rosalbino F, De Negri S, Scavino G, Saccone A. Microstructure and *in vitro* degradation performance of Mg-Zn-Mn alloys for biomedical application. J Biomed Mater Res A 2013; 101(3): 704-711. http://dx.doi.org/10.1007/s10856-009-3956-1

[17] Xu L, Yu G, Zhang E, Pan F, Yang K. *In vivo* corrosion behaviour of Mg-Mn-Zn alloy for bone implant application. J Biomed Mater Res A 2007; 83A(3): 703-711. PMID: 17549695 http://dx.doi.org/10.1002/jbm.a.31273

[18] Zhang S, Zhang X, Zhao C, Li J, Song Y, Xie C, *et al*. Research on an Mg-Zn alloy as a degradable biomaterial. ActaBiomater 2010; 6(2): 626-640. http://dx.doi.org/10.1016/j.actbio.2009.06.028

[19] Yin DS, Zhang EL, Zeng SY. Effect of Zn on mechanical property and corrosion property of extruded Mg-Zn-Mn alloy. T Nonferr Metal Soc 2008; 18(4): 763-768. http://dx.doi.org/10.1016/S1003-6326(08)60131-4

[20] Khan SA, Miyashita Y, Mutohb Y, Sajuri ZB. Influence of Mn content on mechanical properties and fatigue behaviour of extruded Mg alloys. Mater Sci Eng A 2006; (420): 315-321. http://dx.doi.org/10.1016/j.msea.2006.01.091

[21] ASTM Standard E8, in Standard Test Methods for Tension Testing of Metallic Materials, ASTM International, West Conshohocken, PA, 2013. http://dx.doi.org/10.1520/E0008_E0008M

[22] Fischer J, Pröfrock D, Hort N, Willumeir R, Feyerabend F. Improved cytotoxicity testing of magnesium materials. Mater Sci Eng B 2011; 176(11): 830-834. http://dx.doi.org/10.1016/j.mseb.2011.04.008

[23] ISO 10993-5, in Biological evaluation of medical devices, International Organization for Standardization, Geneva, Switzerland, 2009 (E).

[24] Ghali E, Revie RW. General, galvanic, and localized corrosion of magnesium and its alloys, in corrosion resistance of aluminium and magnesium alloys. Quebec: John Wiley & Sons; 2010.

[25] Marsell R, Einhorn TA. The biology of fracture healing. Injury 2011; 42(6): 551-555. http://dx.doi.org/10.1016/j.injury.2011.03.031

[26] Witte F, Kaese V, Haferkamp H, Switzer E, Meyer-Lindenberg A, Wirth CJ, Windhagen H. *In vivo* corrosion of four magnesium alloys and the associated bone response. Biomaterials 2005; 26(17): 3557-3563. http://dx.doi.org/10.1016/j.biomaterials.2004.09.049

[27] Bowen PK, Drelich J, Goldman J. A new *in vitro-in vivo* correlation for bioabsorbable magnesium stents from mechanical behaviour. Mater Sci Eng C Mater Biol Appl 2013; 33(8): 5064-5070. http://dx.doi.org/10.1016/j.msec.2013.08.042

Received on 26-01-2015 Accepted on 04-02-2015 Published on 14-07-2015

DOI: http://dx.doi.org/10.15377/2410-4701.2015.02.01.2